PNAS

Supporting Information for
Tailoring chemical bonds to design unconventional glasses.

Jean-Yves Raty, Christophe Bichara, Carl-Friedrich Schön, Carlo Gatti & Matthias Wuttig.

*Matthias Wuttig

Email: wuttig@physik.rwth-aachen.de

This PDF file includes:

Supporting Information Text

1.Electron Localization and Delocalization Indexes.

In this paragraph, a concise theoretical illustration of the so-called electron localization and delocalization indexes[1], as applied to molecules and periodic and non-periodic solids, is given, followed by some details on the computations performed. The theoretical presentation is, in part, a brief summary of what has been much more extensively reported in Ref. [2]

The average electron population $\mathrm{N}(\Omega)$ of an atom Ω is given by integrating the electron density $\rho(\boldsymbol{r})$ over its basin, $\mathrm{N}(\Omega) = \langle \hat{n}_\Omega \rangle = \int_\Omega \rho(\boldsymbol{r}) d\boldsymbol{r}$. In this work, we have used as atomic basins Ω those defined by the Quantum Theory of Atoms in Molecules (QTAIM) due to Bader[3]. Electron localization and delocalization have a statistical interpretation. They are related to the *variance* and *covariance* of the atomic populations and the corresponding localization and delocalization indices, LI and DI, are respectively given by

$$\mathrm{LI}(\Omega) = \mathrm{N}(\Omega) - Var(\hat{n}_\Omega) = \langle \hat{n}_\Omega \rangle - (\langle \hat{n}_\Omega{}^2 \rangle - \langle \hat{n}_\Omega \rangle^2) \qquad (1)$$

$$\mathrm{DI}(\Omega, \Omega') = -2\mathrm{Cov}\,(n_\Omega, n_{\Omega'}) = -2(\langle \hat{n}_\Omega \hat{n}_{\Omega'} \rangle - \langle \hat{n}_\Omega \rangle \langle \hat{n}_{\Omega'} \rangle) \qquad (2)$$

where $\mathrm{N}(\Omega) \geq \mathrm{LI}(\Omega) \geq 0$ and $\mathrm{DI}(\Omega, \Omega') \geq 0$. For an atom Ω with electrons perfectly localized within Ω, $\mathrm{LI}(\Omega) = \mathrm{N}(\Omega)$ and $\mathrm{DI}(\Omega, \Omega') = 0$ for all Ω'. The properties of variance and covariance require that $\mathrm{N}(\Omega) = \mathrm{LI}(\Omega) + \frac{1}{2} \sum_{\Omega \neq \geq \Omega'} \mathrm{DI}(\Omega, \Omega')$, for every atom Ω in the system. Hence, the average number of electrons in atom Ω can be rigorously partitioned into those that are localized, $\mathrm{LI}(\Omega)$, and those that are *shared*.

The average values in the equations 1 and 2 are calculated by integrating the relevant one- and two-particle densities, namely the electron density $\rho(\boldsymbol{r})$ and the pair density $\pi(\mathbf{r}_1,\mathbf{r}_2)$. The latter may be written in terms of a product of independent electron densities and of the exchange correlation density,

$$\pi(\mathbf{r}_1,\mathbf{r}_2) = \rho(\mathbf{r}_1)\rho(\mathbf{r}_2) - \varrho_{exc}(\mathbf{r}_1, \mathbf{r}_2) \qquad (3)$$

where ϱ_{exc} is a purely non-classical term measuring the deviation of the pair density from the independent-electron distribution. In a Hartree-Fock (HF) calculation the exchange-correlation density contains only the exchange contribution $\varrho_{exc}(\mathbf{r}_1, \mathbf{r}_2) = \gamma(\mathbf{r}_1, \mathbf{r}_2)\gamma(\mathbf{r}_2, \mathbf{r}_1)$ where $\gamma(\mathbf{r}_1, \mathbf{r}_2)$ is the one-electron density matrix, $\gamma(\mathbf{r}_1, \mathbf{r}_2) = \sum_i^{occ.orb.} \lambda_i^2 \psi_i^*(\mathbf{r}_1)\psi_i(\mathbf{r}_2)$, and where λ_i is the occupation number of the occupied orbital ψ_i. In a Kohn-Sham (KS) DFT calculation, only $\rho(\boldsymbol{r})$ is available, but ϱ_{exc} is approximated by replacing ψ_i with the KS orbitals. This is a customarily done approximation yielding DIs that are quantitatively similar to the HF ones and that are deemed to be still chemically meaningful in all those situations where strong correlation effects can be ignored [4] .

The LI and DI are given by the following expressions in terms of ϱ_{exc}

$$\mathrm{LI}(\Omega) = \mathrm{LI}(\Omega, \Omega) = \int_\Omega \int_\Omega \varrho_{exc}(\mathbf{r}_1, \mathbf{r}_2) d\mathbf{r}_1 d\mathbf{r}_2 \qquad (4)$$

$$\mathrm{DI}(\Omega, \Omega') = 2 \int_\Omega \int_{\Omega'} \varrho_{exc}(\mathbf{r}_1, \mathbf{r}_2) d\mathbf{r}_1 d\mathbf{r}_2 \qquad (5)$$

and it may be easily shown that for an HF calculation (hence, with approximation, also for a KS one, see above)

$$\int_{\Omega}\int_{\Omega'} \varrho_{exc}(\mathbf{r}_1,\mathbf{r}_2)d\mathbf{r}_1 d\mathbf{r}_2 = \sum_{ij} S_{ji}^{\Omega} S_{ij}^{\Omega'} \qquad (6)$$

where the S_{ij}^{Ω} are the matrix elements of the atomic domain Ω overlap matrix,

$$S_{ij}^{\Omega} = \int_{\Omega} \lambda_i \lambda_j \psi_i^*(\mathbf{r}_1)\psi_j(\mathbf{r}_1)d\mathbf{r}_1 \qquad (7).$$

Thus, the S_{ij}^{Ω} are the key ingredients to evaluate both LIs and DIs. While the atomic domain overlap matrices are complex Hermitian matrices whose elements depend on the particular set of orbitals that have been adopted to describe a system, Eq. 6 gives rise to the elements $\Omega\Omega'$ of a real symmetric matrix that is invariant to orbital rotations and so are as a consequence both the LI and the DIs.

Evaluation of Eq 4 and 5 is easily affordable for molecular systems, but becomes instead extremely cumbersome in the solid state, because the number of atomic domain overlap matrices in infinite periodic solids makes their calculation much more challenging and heavier.

Baranov and Kohout[5] and later Golub and Baranov[6] have proposed a viable, yet computationally demanding approach, to evaluate LIs and DIs in condensed systems in the context of augmented-plane-wave and of projector-augmented-wave (PAW) wave functions, respectively. Both these approaches use Bloch orbitals or states $\psi_{nk}(\mathbf{r})$ in the calculation of the atomic domain overlap matrices

$$\psi_{nk}(\mathbf{r}) = u_{nk}(\mathbf{r})\boldsymbol{e}^{\boldsymbol{ik}\cdot\mathbf{r}} \qquad (8)$$

written as a truncated expansion in augmented plane-waves. In Eq. 8 $\boldsymbol{k}$ is a vector in the first Brilouin zone, *n* is the band index and the Bloch states are separated into a periodic part $u_{nk}(\mathbf{r})$ and a phase $e^{i\boldsymbol{k}\cdot\mathbf{r}}$ thanks to Bloch's theorem. In the present work we have adopted, instead, a more recent and much faster approach due to Otero-de-la-Roza, Martín Pendás and Johnson[2] that adopts Maximally Localized Wannier Functions[7,8] to bypass the calculation of all atomic overlaps related to functions whose centers are sufficiently far apart. Wannier functions[9] are real-space alternatives of Bloch states and are obtained from these latter through the transformation

$$w_{n\boldsymbol{R}}(\mathbf{r}) = \frac{V}{(2\pi)^3}\int \psi_{nk}(\mathbf{r})e^{-i\boldsymbol{k}\cdot\boldsymbol{R}}\,d\boldsymbol{k} \qquad (9)$$

where the integration is over the first Brillouin zone and **R** is a real space vector**.** Wannier functions constitute a representation of a periodic system's electronic wave function that is completely equivalent to the one obtained using extended Bloch states. MLWFs are the result of a peculiar Wannier transformation (Eq. 9) where the Bloch states are rotated

$$\tilde{\psi}_{nk}(\mathbf{r}) = \sum_m \boldsymbol{U}_{nm}^{\boldsymbol{k}}\,\psi_{mk}(\mathbf{r}) = e^{i\boldsymbol{k}\cdot\boldsymbol{r}}\sum_{\boldsymbol{m}} \boldsymbol{U}_{nm}^{\boldsymbol{k}}\,u_{mk}(\mathbf{r}) \qquad (10)$$

so that the combined spread of all the resulting Wannier functions is minimized[7]. MLWFs are the solid-state analogue of the Foster and Boys localized molecular orbitals[10]. Atomic domain overlap matrices in terms of Wannier functions (either standard or MLWFs) are given by

$$S_{n\boldsymbol{R},n'\boldsymbol{R}'}^{\Omega+\boldsymbol{R}''} = \int_{\Omega+\boldsymbol{R}''} w_{n\boldsymbol{R}}^*(\mathbf{r})w_{n'\boldsymbol{R}'}(\mathbf{r})d\mathbf{r} \qquad (11)$$

where $\Omega + \boldsymbol{R}''$ is an atom Ω translated by lattice vector $\boldsymbol{R}'', n\ and\ n'$ are band indices, and $\boldsymbol{R}$, $\boldsymbol{R}'$ $\boldsymbol{R}''$ are lattice vectors. From a comparison of Eq. 11 and Eq. 7 it is clear that the number of atomic overlaps to be calculated for a periodic solid becomes much higher than in the molecular case. As a clarifying example, a few billions of atomic overlaps are required to calculate all of the DIs in the

urea crystal, while only a few thousands of them are needed for the *in vacuo* urea molecule. To be able to calculate the DIs even for the simplest solids, one has to avoid the calculation of as many atomic overlaps as possible and to compute the non-negligible overlap integrals very efficiently**.** Using MLWFs a significant number of atomic overlap integrals can be discarded *a priori* and equated to zero as the integral in eq. 11 is assumed to give a negligible contribution if the distance between the MLWFs centers is high enough (for technical/computational details see Ref. [2]).

2. DI vs distance in glasses

Figure S1 here

3. Relation between aging and localization in GeTe

Figure S2 here

4. Extended discussion of the relationship between structure and bonding

In the main manuscript, Figure 1 displays the number of electrons shared ES, which is twice delocalization index (DI) value, against internuclear Ge-Te distances for the most stable GeTe amorphous structure. A large number of different DI values is obtained for the different atomic distances found in the glass. For the sake of comparison, data at the two Ge-Te distances found in the crystalline GeTe structure (at 0 K) are also indicated. As expected the electron sharing is decreasing with increasing atomic separation and decreasing covalent character of the bonding. This figure quantifies the common belief that the bond length scales with the bond strength. A similar behavior was recently reported by Lee and Elliott[12] for a number of chemical-bonding indicator data, calculated at the Ge-Te and Sb-Te homopolar bond critical points (BCPs) in simulated models of amorphous and crystalline GST. Common to the present study and the one by Lee and Elliott it is the fact that the property data for the crystal structures exactly fall on the property evolution curves obtained from the wider range and (much) more numerous datapoints of the related amorphous structures. This observation brought Lee and Elliot to conclude that the "surprising similarity (of properties) indicates that interatomic interactions in c-GST are indistinguishable from (some of) those in a-GST; more precisely, chemical-bonding interactions in c-GST belong to a subgroup of the broad spectrum of interactions existing in a-GST, but are not a different type of interaction to those present in a-GST". We are indeed not surprised by the similarity of properties of bonding in amorphous and crystalline structures when they are evaluated *at a common geometry*. This is purely a consequence of the local character of the properties being examined. Those properties considered by Lee and Elliot are local in nature since they refer to a precise point, the BCP, taken as the most representative point along the bond path joining the two bonded nuclei[3]. The DIs, despite being the result of an integration of the exchange correlation density over the two atomic basins of the bonded atoms, are known to be also fundamentally local in character because of the short-range nature of electron delocalization[13].

Figure S3 here

It is hence no surprise that the same (local) atomic arrangement in the glass and the crystal is accompanied by the same chemical bonding descriptors. This is the essence of the Zachariasen conjecture, the similarity of chemical bonding in the glass and the crystal leads to a similarity in atomic arrangement. Yet, for glasses like GeTe and $GeSb_2Te_4$, is has been long known that the atomic arrangement differs considerably from the corresponding crystal. This can only be explained if there are significant differences in bonding between the glass and the crystal. Figure 1 shows convincingly that this is indeed the case.

It is the peak(s) height, position and width of interatomic distance distributions that drastically distinguishes amorphous and crystal structures, thus leading to their quite distinct "average" bonding features and properties. In particular, differently from the amorphous case, the peaks of crystal GeTe have zero width and positions that almost correspond to the larger and lower internuclear distances found for the low and large internuclear distance groups in the amorphous

structure. As a consequence, the two distinct peaks, having the same height but quite different DI values (0.25 and 0.65) in the crystal (Fig. S2 and S3), are replaced by two very broad and shallow peaks in the amorphous structure. Each of them has DI values distributed in a range that is roughly as large as it is the DI difference between the two distinct peaks in the crystal.

5. Measuring the deviation from the Zachariasen character

To define an order parameter NZ characterizing the difference between crystal and amorphous local environments, we use the distributions of the first distances around each kind of atom obtained from Molecular Dynamics simulations. These distributions overlap (Figure 2a, Figure S4a-f) and their averages (Figure 2b, c) and fluctuations are used to calculate NZ in the following way. For each atom of species j in the structure, we identify its N_i first neighbors, and create N_i histograms of these distances, once they are sorted. NZ is defined as a sum of partial contributions Z_j from the N_{sp} atomic species:

$$NZ = \sum_{j=1}^{N_{sp}} c_j \, Z_j$$

$$Z_j = S\left\langle \frac{1}{N_j} \sum_{i=1}^{N_j} \left(\frac{d_i^A - d_i^C}{d_i^C} \right)^2 \right\rangle^{1/2}$$

c_j is the concentration of species j, S is a scaling factor to set NZ between 0 and 1 ($S = 25$ here). We choose N_j =6 for all systems, although SiO_2 and $GeSe_2$ are tetrahedrally bonded crystals whereas GeSe, GeTe, $GeSb_2Te_4$ are octahedrally bonded (rhombohedral and orthorhombic structures). In any case, the inclusion of the 5th and 6th neighbor contribution in SiO_2 and $GeSe_2$ is slightly increasing the value of NZ (see Table S6.2). The terms in the sum are the squared relative difference of the averaged i^{th} bond lengths (d_i^C, d_i^A) between crystal and amorphous. The values of the parameters obtained from Molecular Dynamics and resulting Z_j and the contributions to NZ are given in Supplementary Tables S2 and S3.

6. Neighbors distributions in glasses vs crystals.

Here we present the distance analysis for all 6 systems and all species. In each case, we plot on the top panel the distributions of the first six normalized distances around a given species in both the glassy (orange) and crystalline (green) phases. From these, the average distances shown in the corresponding bottom panel have been computed.

Figure S4 a-f here

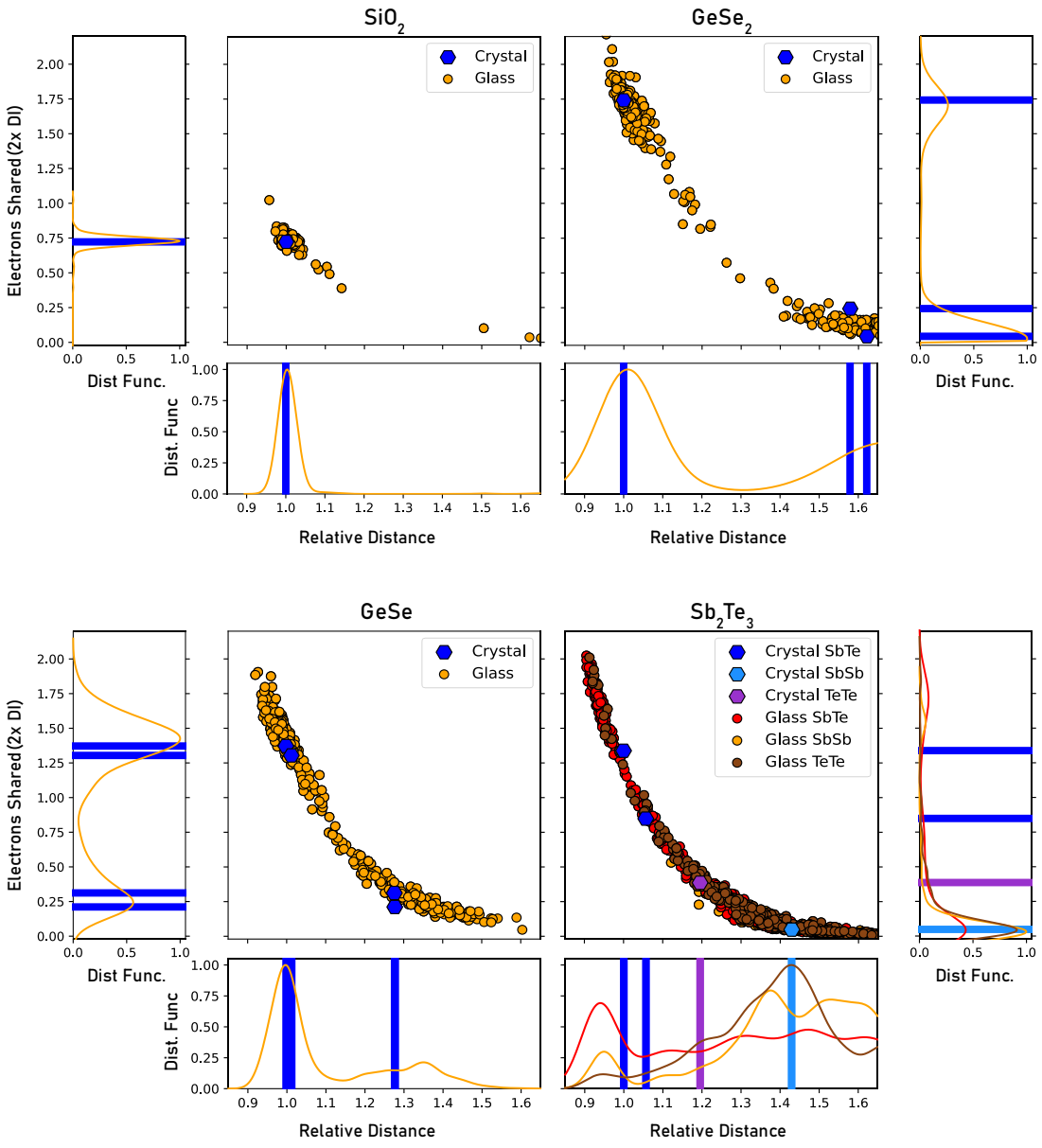
SiO2
GeSe2
GeSe
Sb2Te3
Crystal
Glass
Crystal SbTe
Crystal SbSb
Crystal TeTe
Glass SbTe
Glass SbSb
Glass TeTe
Electrons Shared (2x DI)
Dist Func.
Dist. Func
Relative Distance

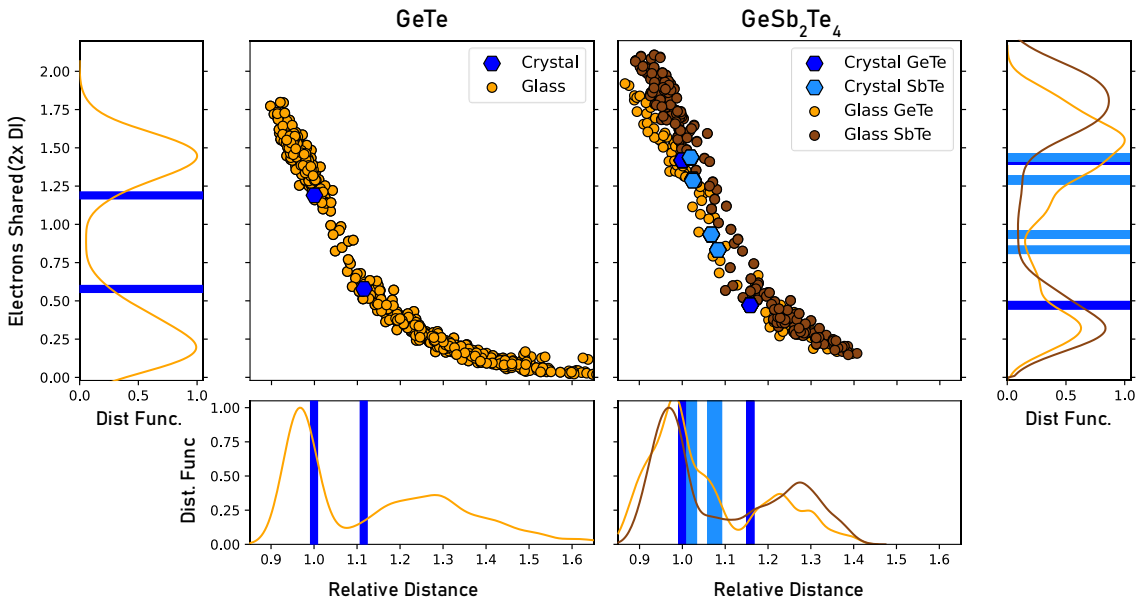

Fig. S1. For each system, the square panel shows the delocalization index (DI) values as a function of inter-atomic distance (rescaled to the shortest corresponding distance in the crystal.). The vertical and horizontal panels show the distribution of DI and of distances, respectively, the values for the crystal being indicated by the bars. The difference between distributions in the crystal and in the amorphous appear clearly for GeTe and GeSb2Te4 (GST). In the case of GeSe, both distance and DI distributions have peaks located very close to those of the crystal, as it is observed for GeSe2. Upon ageing, the DI distribution of glassy GeTe evolves and becomes even more distinct from the crystal as illustrated in Figure S2.

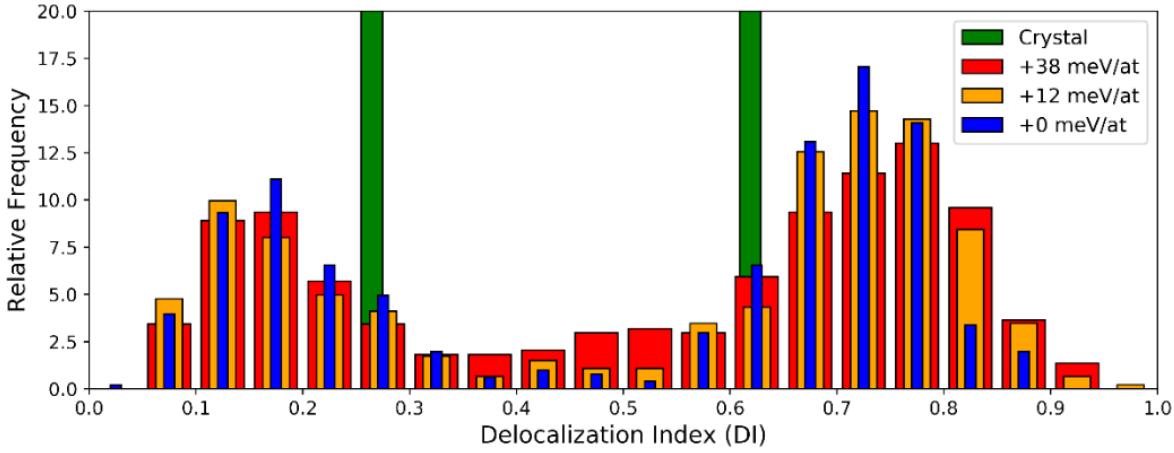

Fig. S2. Detailed distributions (vertical panels in Fig 1B) for various GeTe amorphous models. Upon ageing, the total energy (given in the legend) of the structure decreases[11], the evolution of the distribution is characterized by better defined peaks in the lowest energy structure (around DI=0.18 and DI=0.73) with a clear decrease in bonds with DI 0.35-0.55 (0.7 to 1.1 electron share). This subtle variation is not linked with the small proportion of homopolar bonds. See Ref. [11] for a detailed description of the structural evolution.

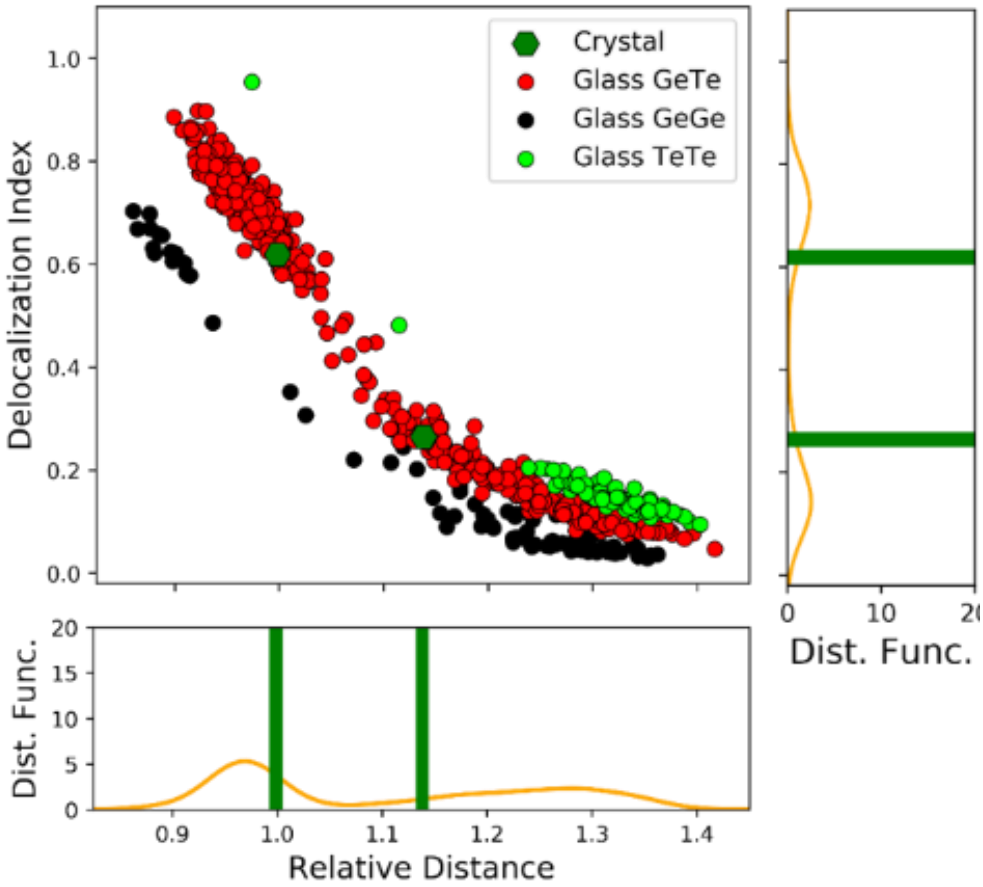

Fig. S3. Delocalization Index (DI) values (first six neighbors) for low energy amorphous GeTe. Ge-Te, Ge-Ge and Te-Te bonds are plotted in red, black and green, respectively. The distributions of the DIs and of the distances values are plotted on the right and below the main panel. The green bars indicate the crystal values. One can notice the large deviation between average DI in the amorphous and in the crystal, linked with smaller interatomic distances.

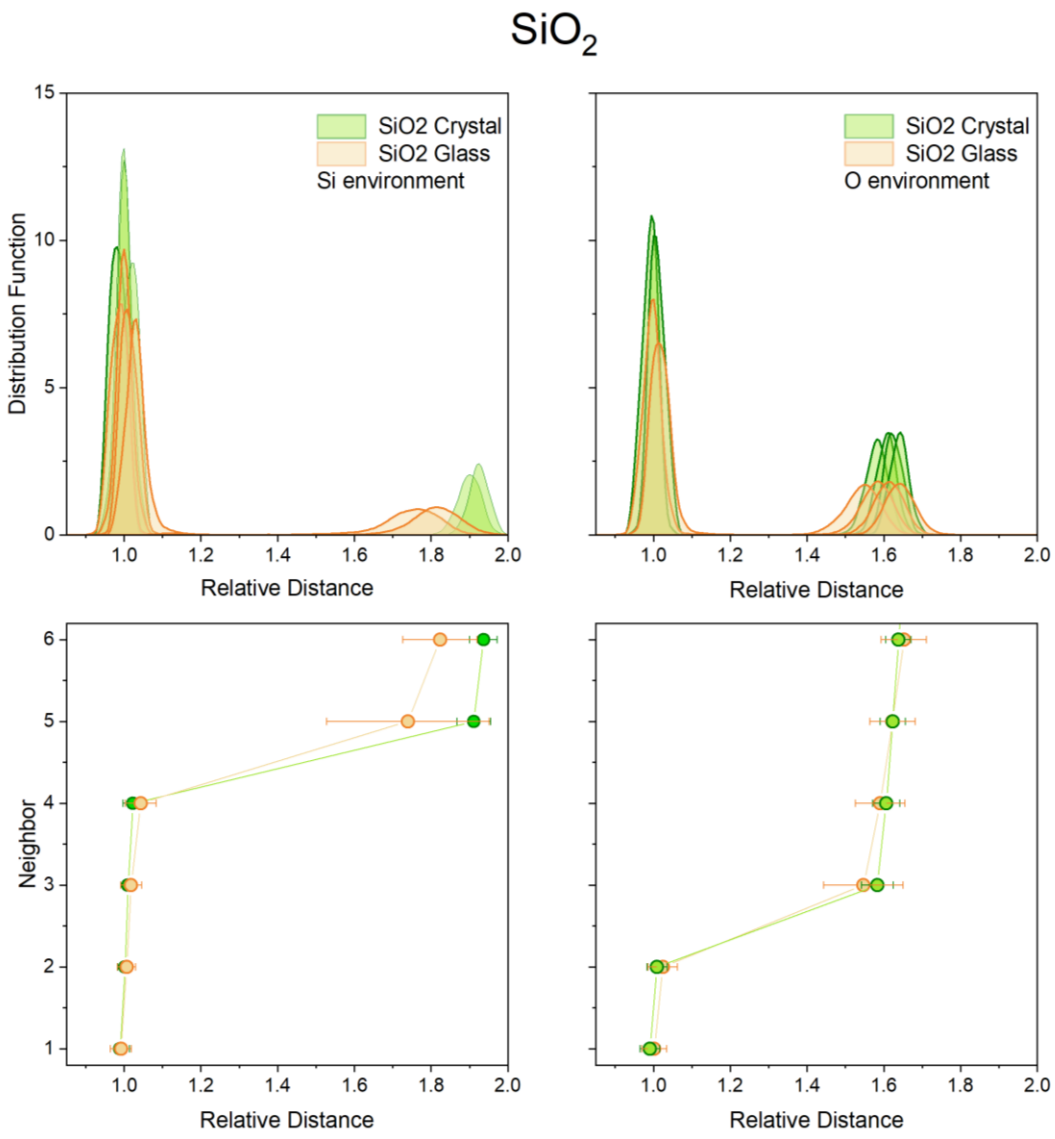

Fig. S4.a. The SiO_2 glass is almost perfectly tetrahedrally coordinated. Only angular fluctuations are responsible for the broader/shorter 5th and 6th distance distributions.

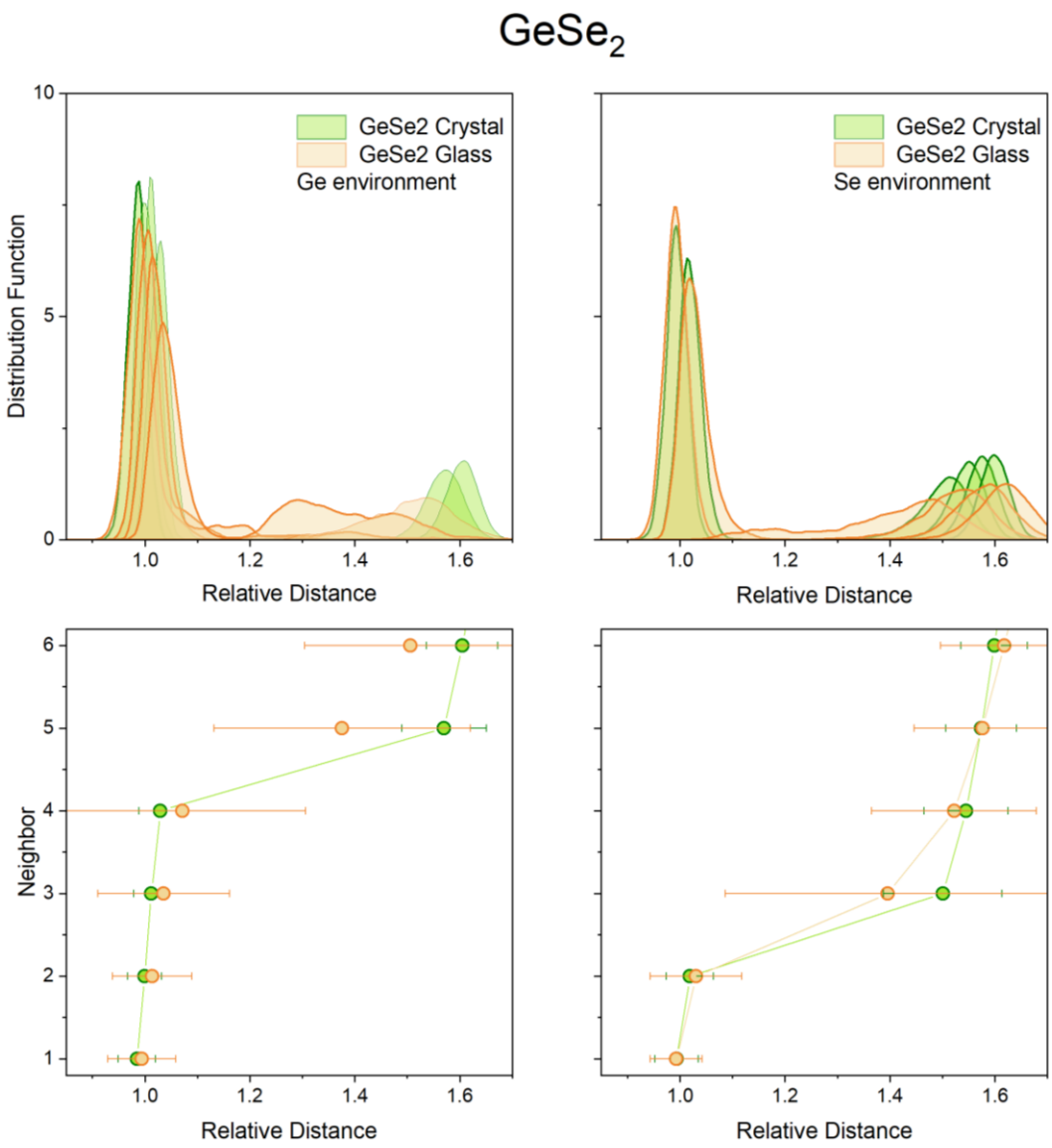

Fig. S4.b. In glassy $GeSe_2$, the tetrahedral nature of the local order around Ge atoms is preserved, as well as the two-fold coordination of the Se atoms. Coordination defects (linked to the presence of a few homopolar bonds) are responsible for the larger distribution of the 4th and 5th neighbor of Ge atoms, and the 3rd neighbor distribution for O atoms.

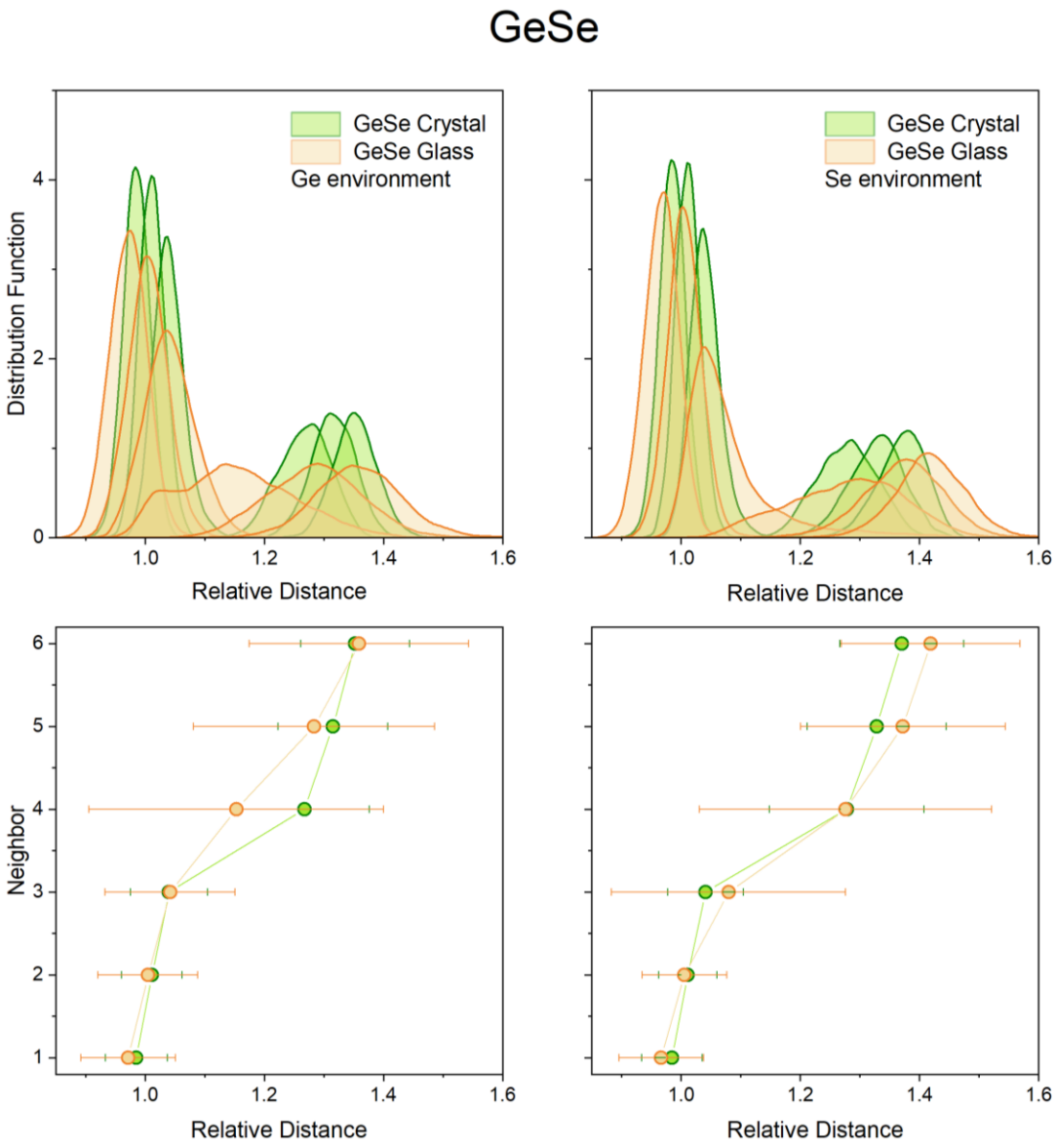

Fig. S4.c. The GeSe crystal is orthombic and the structure derives from a Peierls distortion of a cubic structure. As a consequence, shorter and longer bonds are found and the local Ge and Sb environment is a '2+1 / 1+2' distorted octahedron. In the glass, the local order appears quite similar, with a '3+3' effective coordination of both Ge and Sb atoms. The presence of a few homopolar Ge-Ge bonds causes the broader distribution of the 4th Ge neighbor (bimodal distribution).

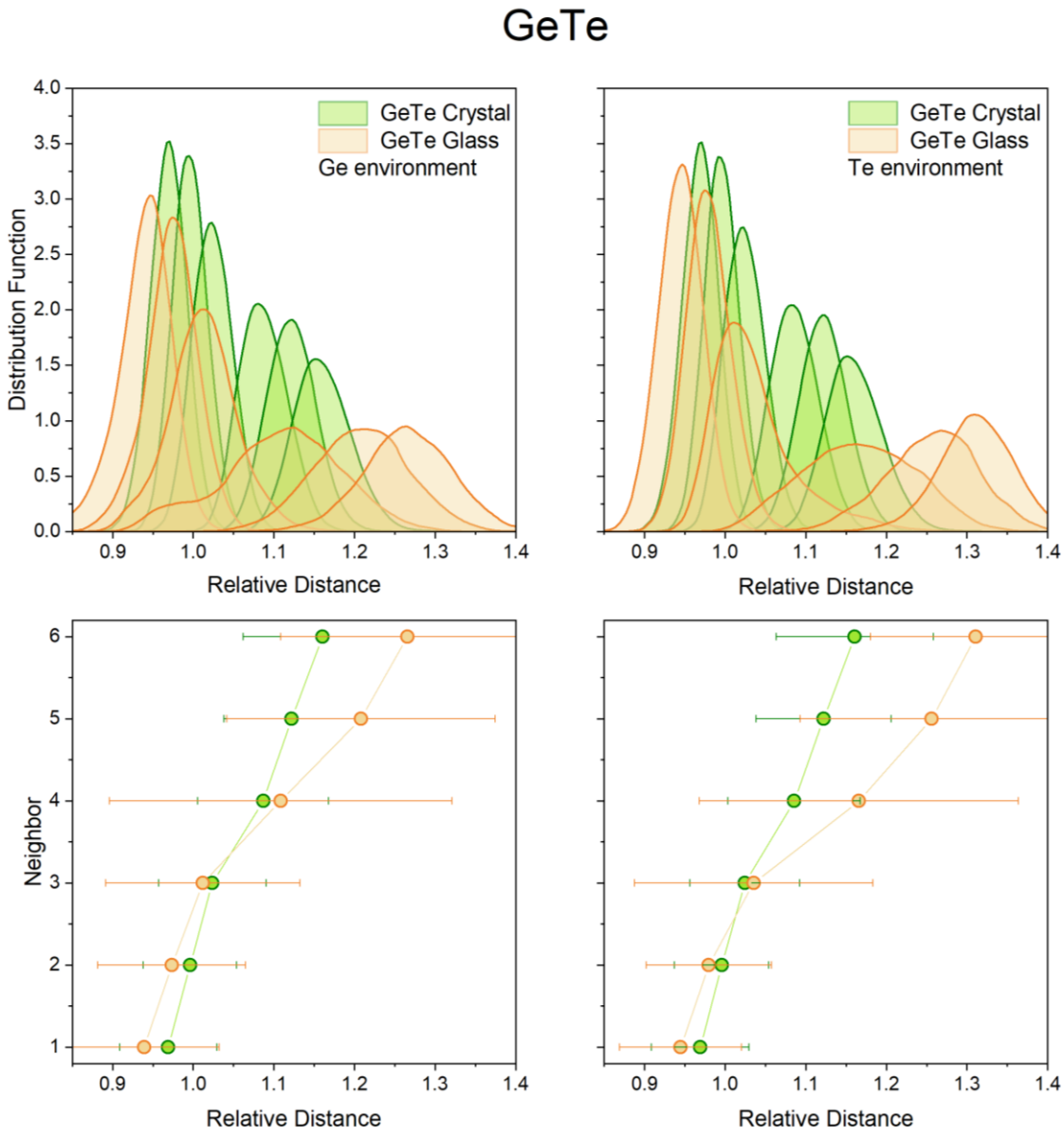

Fig. S4.d. The R-3m crystalline structure of GeTe corresponds to a '3+3' coordination in a distorted octahedral geometry. In the amorphous (as described in Ref. [11], for instance), the dominant order remains octahedral, but with much larger Peierls distortion ratio (the short distances are shorter, and the long ones are longer in the amorphous phase). Furthermore, the coordination number is smaller (tends toward 3 for both Ge and Te atoms). Here, the broader 4th neighbor distribution around Ge atoms is due to a bimodal distribution (few tetrahedral Ge atoms, with Ge-Ge homopolar bonds).

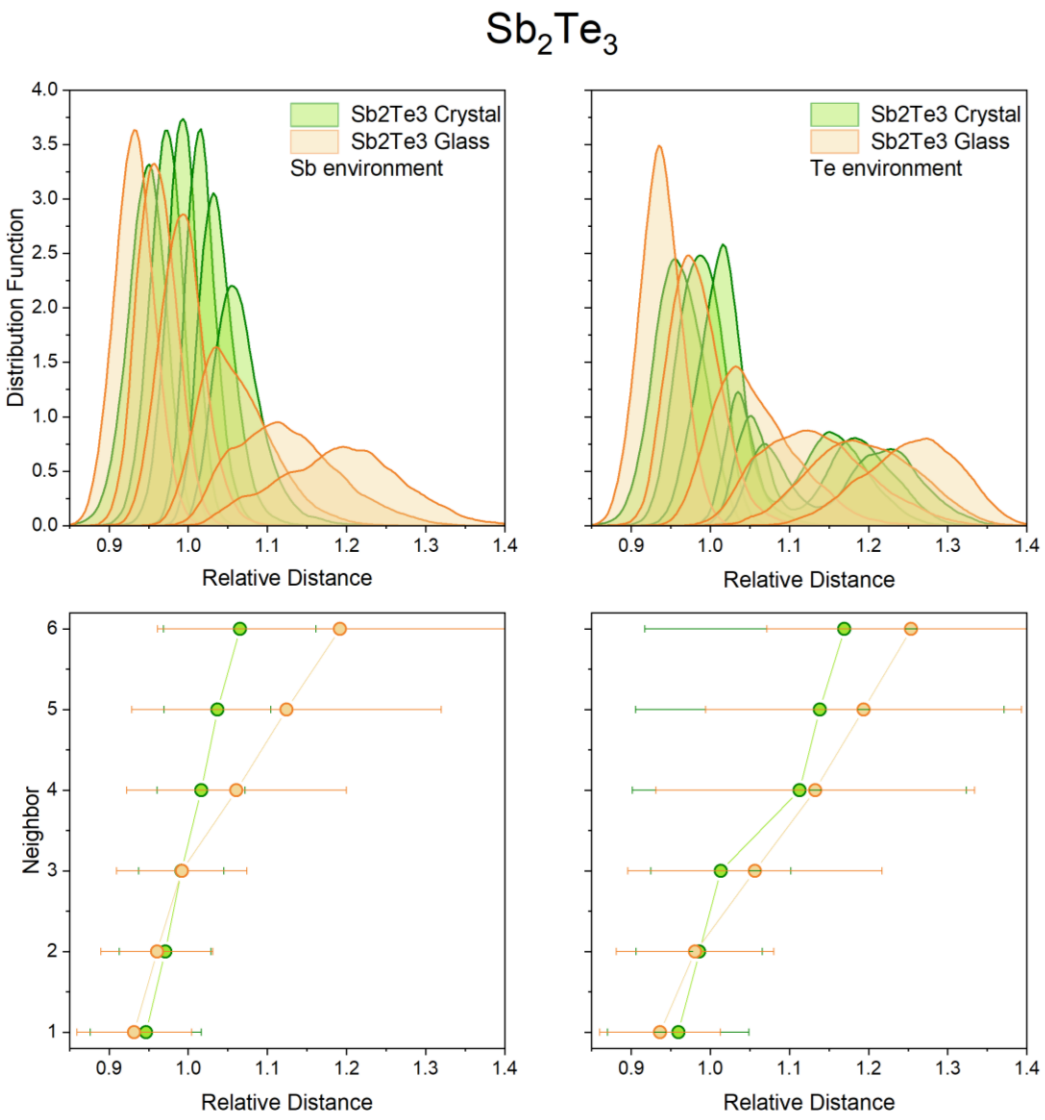

Fig. S4.e. In the R-3m crystalline structure of Sb2Te3, each atom is locally octahedrally bonded. Around Sb atoms, 6 equal bonds are found, whereas two types of Te sites exist. 1/3 of the Te atoms have '3+3' Sb neighbors, the remaining 2/3 of Te having 3 short Sb-Te bonds and 3 longer Te-Te bonds.The structure of the glass is very different. For the Sb atoms, the coordination is much lower with 3 short Sb-Te bonds. Te atoms also have a lowered average coordination.

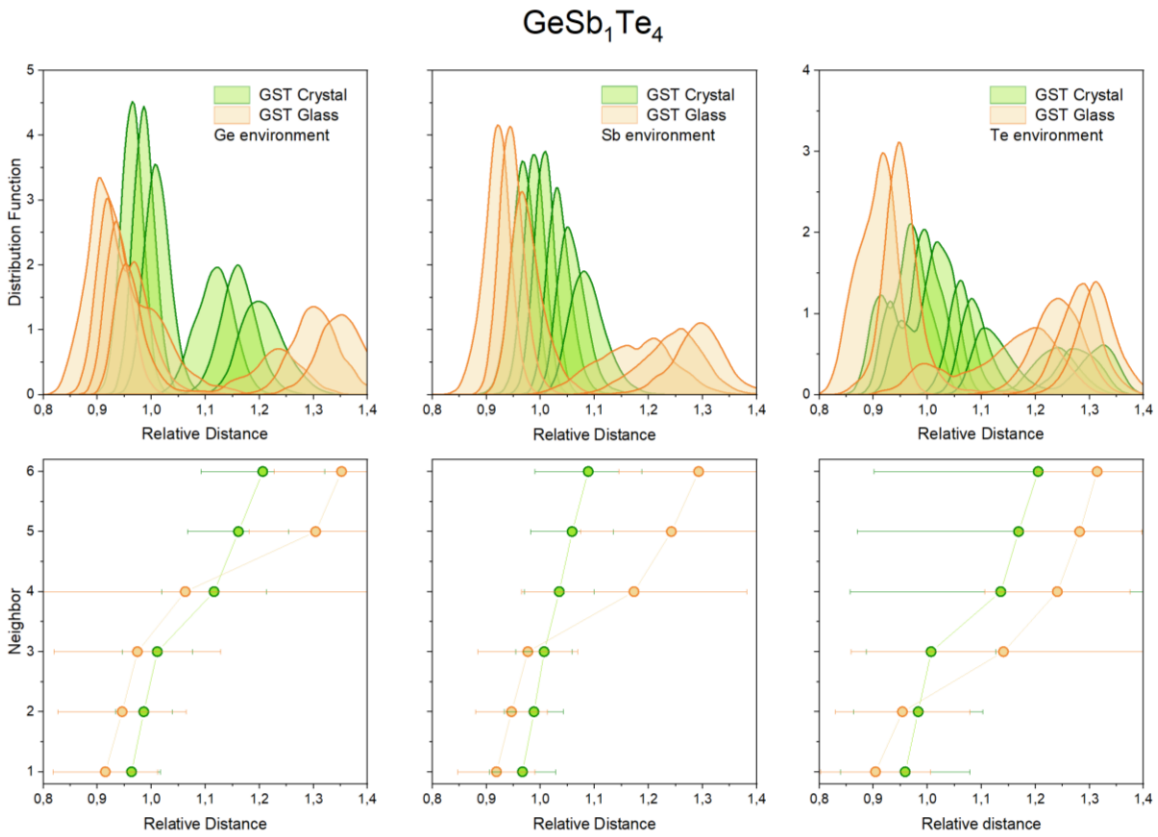

Fig. S4.f. The R-3m crystalline structure of $GeSb_2Te_4$ is layered with local octahedral order. Due to Peierls distortions, Ge atoms have a '3+3' coordination, Sb have 6 first neighbors and two Te sites exist as for Sb_2Te_3.
In the glass, Ge atoms have 3 or 4 first neighbors (broad 4^{th} neighbor, and a bimodal distribution due to the presence of a few homopolar bonds). Sb atoms are 3-fold coordinated and Te atoms are either 2- or 3-fold coordinated.

Table S1. Structural data for glasses and crystals at finite T.

Interatomic distance (maximum of the partial g(r)), coordination number (cutoff from minimum of partial g(r) in column 1), representative angle (width from a gaussian fit). All amorphous and crystal values are obtained from averaging over trajectories at 300K.

	R1 (Å)	**R1 (Å, litt.)**	**Coordination number (*cutoff Å*)**	**Z (Litt)**	**Angle (σ)**
SiO_2 Glass	SiO: 1.63 SiSi: 2.99 OO: 2.63	[14] SiO:1.62 SiSi:3.1	Si : Z=4.01 *(2.0Å)* O: Z=2.01	[14] Si: Z=4 O: Z=2 O-Si-O 109°	O-Si-O 109° (13) 100% Corner Sharing
SiO_2 Crystal 300K	SiO: 1.62 SiSi: 3.14 OO: 2.64		Si : Z=4 (*2.0Å*) O : Z=2		O-Si-O: 109° (7) 100% Corner Sharing
$GeSe_2$ Glass	GeSe: 2.42 GeGe: 2.52 SeSe: 2.36	[15,16] 2.37, 2.36 2.45, 2.42 2.36, 2.32	Ge : Z=3.89 (*3.14Å*) 0.23Ge+3.65Se Se : Z=2.10 1.83Ge+0.27Se Ge : 89% Z=4 10% Z=3 Se : 89% Z=2 10% Z=3	[16] Ge : Z=3.96 0.25Ge+3.71Se Se : Z=2.05 1.86Ge+0.20Se	Ge-Se-Ge : 80° (12)+100°(8) Se-Ge-Se : 109° (21)
$GeSe_2$ Crystal 300K (Ortho.)	GeSe: 2.41		Ge : Z=4 (*2.95Å*) Se : Z=2		Ge-Se-Ge 100° (8) Se-Ge-Se 109° (17)
GeSe Glass	GeSe: 2.57 GeGe: 3.67 SeSe: 3.81		Ge : Z=3.41 (*3.0Å*) 0.53Ge+2.89Se 58% Z=3 38% Z=4 2% Z=2 Se: Z=2.89 2.89 Ge 74% Z=3 19% Z=2 7% Z=4		Ge-Se-Ge : 89° (29) Se-Ge-Se : 95.0° (18)
GeSe Crystal 300K	GeSe: 2.61 GeGe: 3.60 SeSe : 3.80		Ge : Z=3 (*3.0Å*) Se : Z=3		Ge-Se-Ge : 101° (11) Se-Ge-Se : 94° (8)
Sb_2Te_3 Glass	SbTe: 2.97 TeTe : 4.18	[17] SbTe:2.94	Sb: Z=4.87 (*3.56Å*) 0.78Sb+4.09Te 28% Z=4 44% Z=5	[17] Sb: Z=5.2 (*3.9Å*) 0.6Sb+4.6Te	Sb-Te-Sb 85° (9) Te-Sb-Te 91° (12)

	R1 (Å)	R1 (Å, litt.)	Coordination number (*cutoff Å*)	Z (Litt)	Angle (σ)
		TeTe: 4.25	23% Z=6 Te : Z=3.90 2.73Sb+1.17Te 6% Z=2 30% Z=3 37% Z=4 21% Z=5, 6% Z=6	Te Z=3.5 3.1Sb+0.7Te ~90° angles.	
Sb_2Te_3 Crystal 300K	SbTe: 3.06 TeTe: 3.53		Sb : Z=6.0 (*3.56Å*) Te : Z=5.15 4.0Sb +1.15Te 19% Z=4 24% Z=5 49% Z=6		Sb-Te-Sb 93° (9) Te-Sb-Te 91° (8)
GeTe Glass	GeTe: 2.78 GeGe:2.61 TeTe: 4.02		Ge: Z=3.29 (3.12Å) 0.35Ge+2.94Te 63% Z=3 31% Z=4 4% Z=2 Te: Z=2.96 0.02Ge+2.94Te 72% Z=3 12% Z=4 16% Z=2		Ge-Te-Ge 89° Te-Ge-Te 93° (16)
GeTe Crystal 300K	GeTe: 2.87+3.20		Ge: Z=6 (3+3) (*3.66Å*) Te : Z=3 (3+3)		Te-Ge-Te 94° (8) Ge-Te-Ge 93° (9)
$GeSb_2Te_4$ Glass	GeTe: 2.68 SbTe:2.85 TeTe:4.07	[18] GeTe: 2.61 SbTe: 2.83	Ge:Z=3.48 (*3.26Å*) 0.4Ge+0.3Sb+2.78Te 46% Z=3 51% Z=4 3% Z=2 Sb:3.06 0.2Ge+0.3Sb+2.61Te 92% Z=3 7% Z=4 Te: Z=2.15 0.7Ge+1.31Sb+0.16Te	[19] Ge: Z=3.9 Sb: Z=2.8 Te: Z=2.4 [18] Ge: Z=3.91 Sb: Z=2.91 Te: Z=1.98	Ge-Te-Ge 89°+100° Te-Ge-Te 101°(22) Sb-Te-Sb 95°(17) Te-Sb-Te 96°(18)
$GeSb_2Te_4$ Crystal 300K	GeTe: 2.80 SbTe: 3.02 TeTe: 4.33		Ge: Z=3.05 (*3.05Å*) Sb: Z=6 (*3.63Å*) Te: Z=3.84 (*3.63Å*)		Ge-Te-Ge 99.4° (8) Te-Ge-Te 99.4°(8) Sb-Te-Sb 90.6°(13) Te-Sb-Te 90.5°(9)

Table S2. Partial and total Non Zachariasen parameters for all systems studied

As the NZ parameter is a measure of the difference between amorphous and crystalline local orders, a clear splitting is observed between covalent systems with $NZ \leq 0.4$ and incipient metals with $NZ \geq 0.55$. Averages for GeTe and GST are 0.764 and 0.868, respectively. Among the various structures, that sample labelled GeTe2 has the lowest total energy, corresponding to the smallest proportion of homopolar bonds and tetrahedral defective Ge atoms. This shows that independent of homopolar defective bonds, the GeTe glass has a much larger NZ value than 'regular' Zachariasen glasses.Z1,Z2,Z3 indicate the various species, and ZAv is the value averaged over the various models.

These data are used to produce fig.2, panel d.

System	N_j	Z1	Z2	Z3	Z	*ZAv*
SiO_2	6	0.451	0.143		**0.245**	
$GeSe_2$	6	0.207	0.302		**0.271**	
GeSe	6	0.394	0.267		**0.330**	
Sb_2Te_3	6	0.589	0.564		**0.574**	
GeTe1	6	0.609	0.924		**0.767**	
GeTe2	6	0.527	0.805		**0.666**	
GeTe3	6	0.617	0.982		**0.800**	***0.764***
GeTe4	6	0.720	0.925		**0.823**	
GST124a	6	0.831	1.173	0.805	**0.914**	
GST124b	6	0.592	1.106	0.737	**0.822**	***0.868***

Table S3: Partial contributions to Z_j in covalent systems.

$D_i = \left(\frac{d_i^A - d_i^C}{d_i^C}\right)^2$, with i indicating the neighbor (sorted by increasing distance).

System		D1	D2	D3	D4	D5	D6
SiO_2	**Si**	1.4E-5	1.8E-5	7.4E-5	1.2E-4	8.1E-3	3.4E-3
	O	3.0E-5	8.0E-5	7.6E-4	2.6E-4	4.6E-5	2.2E-6
$GeSe_2$	**Ge**	8.7E-5	2.0E-4	5.3E-4	1.7E-3	1.5E-2	3.8E-3
	Se	7.0E-7	1.3E-4	4.9E-3	2.2E-4	2.6E-6	1.4E-4
GeSe	**Ge**	1.9E-4	4.3E-5	3.8E-6	8.1E-3	5.8E-4	2.2E-5
	Se	3.3E-4	3.1E-5	1.4E-3	2.3E-6	1.1E-3	1.2E-3
Sb_2Te_3	**Sb**	7.4E-4	4.2E-4	6.1E-5	1.2E-3	5.5E-3	1.2E-2
	Te	1.1E-3	2.0E-4	1.2E-3	1.8E-3	4.4E-3	9.5E-3
GeTe1	**Ge**	2.2E-3	2.1E-3	2.2E-3	5.6E-4	6.4E-3	8.0E-3
	Te	1.3E-3	1.2E-3	1.8E-5	1.1E-2	1.9E-2	1.7E-2
GeTe2	**Ge**	9.2E-4	5.2E-4	1.3E-4	4.3E-4	5.9E-3	8.1E-3
	Te	6.5E-4	2.6E-4	1.3E-4	5.5E-3	1.4E-2	1.6E-2
GeTe3	**Ge**	3.4E-3	2.5E-3	2.0E-3	1.4E-3	5.1E-3	7.6E-3
	Te	1.8E-3	8.2E-4	1.1E-3	1.3E-2	1.9E-2	1.9E-2
GeTe4	**Ge**	5.8E-3	4.0E-3	3.2E-3	2.1E-3	5.8E-3	8.9E-3
	Te	2.6E-3	1.2E-3	1.3E-3	1.2E-2	1.7E-2	1.5E-2
GST124a	**Ge**	3.0E-3	2.2E-3	2.3E-3	2.2E-3	1.6E-2	1.4E-2
	Sb	2.5E-3	2.1E-3	1.3E-3	1.5E-2	2.7E-2	3.1E-2
	Te	3.3E-3	1.2E-3	1.5E-2	1.1E-2	1.1E-2	9.3E-3
GST124b	**Ge**	1.3E-3	9.7E-4	6.0E-4	3.3E-4	7.9E-3	9.2E-3
	Sb	2.2E-3	1.9E-3	9.9E-4	1.2E-2	**2.4E-2**	**2.9E-2**
	Te	2.9E-3	1.3E-3	1.1E-2	8.2E-3	**1.0E-2**	**8.7E-3**

Table S4. Properties tables

These data are used to produce fig.3. Z* is the Born effective charge of the cation (averaged for the amorphous phase) obtained as one third of the trace of the Z* tensor, given for Sb atoms in GST). Emax and Hmax are the position (in energy) and height of the first peak of the imaginary dielectric function. Vmax is the maximal vibration frequency. The effective coordination number Econ is given for the cation (Sb in Sb containing cases). (*) In the DFT calculations, crystalline Sb_2Te_3 being metallic and glassy Sb_2Te_3 having close to 0 eV gap, such that dielectric properties have not been obtained. Hence, for Sb_2Te_3 the experimental data from Ref.[20] were used.

	ε_∞	Z* (e)	$E(\varepsilon_2^{Max})$ (eV)	ε_2^{Max}	vmax(THz)	ECoN
SiO_2 glass	2.54	3.28	10.12	2.58	40.33	3.98
SiO_2 crystal	2.22	3.59	9.67	2.89	32.94	4
$GeSe_2$ glass	6.20	2.20	5.03	7.40	9.53	3.82
$GeSe_2$ crystal	5.57	2.51	4.03	10.56	9.46	4
GeSe glass	12.10	2.26	3.36	13.87	8.54	3.54
GeSe crystal	14.22	3.10	2.94	21.52	6.68	3.09
Sb_2Te_3 glass	21*	4*	1.64	26.18	5.45	4.32
Sb_2Te_3 crystal	41*	11*	1.31	90.15	4.83	5.84
$Ge_1Sb_2Te_4$ glass	24.30	2.43	1.85	20.75	7.50	3.54
$Ge_1Sb_2Te_4$ crystal	52.36	6.80	1.59	73.19	5.78	4.64
GeTe glass	23.07	2.24	2.27	23.75	8.60	3.53
GeTe crystal	75.91	5.26	1.36	93.12	3.94	5.18

SI References

1. X. Fradera, M.A. Austen, R.W.F. Bader, The Lewis model and beyond. *J. Phys. Chem. A* **103**, 304-314 (1999)
2. A. Otero-de-la-Roza, A.P. Pendás, E.R. Johnson, Quantitative electron delocalization in solids from maximally localized Wannier functions. *J. Chem. Theory Comput.* **14**, 4699-4710 (2018)
3. R. F. W. Bader, Atoms in molecules: A quantum theory (Clarendon Press, Oxford, 1990)
4. X. Fradera, J. Poater, S. Simon, M. Duran, M. Solà, Electron-pairing analysis from localization and delocalization indices in the framework of the atoms-in-molecules theory. *Theor. Chem. Acc.* **108**, 214-224 (2002)
5. A.I. Baranov, M. Kohout, Electron localization and delocalization indices for solids. *J. Comput. Chem.* **32**, 2064−2076 (2011)
6. P. Golub, A.I. Baranov, Domain overlap matrices from plane-wave-based methods of electronic structure calculation. *J. Chem Phys*. **145**, 154107 (2016)
7. N. Marzari, D. Vanderbilt, Maximally localized generalized Wannier functions for composite energy bands. Phys. Rev. B, **56**, 12847 (1997)
8. N. Marzari, A.A. Mostofi, J.R. Yates, I. Souza, D. Vanderbilt, Maximally localized Wannier functions: Theory and applications. *Rev. Mod. Phys.* **84**, 1419 (2012)
9. G.H. Wannier, The structure of electronic excitation levels in insulating crystals. *Phys. Rev*. **52**, 191 (1937)
10. J.M. Foster, S. Boys, Canonical configurational interaction procedure. *Rev. Mod. Phys.* **32**, 300 (1960)
11. J.Y. Raty *et al.,* Aging mechanisms in amorphous phase-change materials. *Nat. commun.* **6**, 1-8 (2015)
12. T.H. Lee, S.R. Elliott, Chemical Bonding in Chalcogenides: The Concept of Multicenter Hyperbonding. *Adv. Mater*. **32**, 2000340 (2020)]
13. A. Gallo-Bueno, M. Kohout, E. Francisco, A.M. Pendás, Localization and Delocalization in Solids from Electron Distribution Functions*, J. Chem. Theory Comput*. **18**, 4245-4254 (2022)
14. D.A. Keen, M.T.T. Dove, Local structures of amorphous and crystalline phases of silica, SiO2, by neutron total scattering. *J. Phys.: Condens. Matter* **11**, 9263 (1999)
15. C. Massobrio, A. Pasquarello, Structural properties of amorphous GeSe2. *J. Phys.: Condens. Matter*.**19**, 415111 (2007)
16. P.S. Salmon, I. Petri, Structure of glassy and liquid GeSe2. *J. Phys.: Condens. Matter* **15**, S1509 (2003)
17. K. Konstantinou, J. Mavračić, F.C. Mocanu, S.R. Elliott, S. R. Simulation of Phase-Change-Memory and Thermoelectric Materials using Machine-Learned Interatomic Potentials: Sb2Te3. *Phys. Status Solidi B* **258**, 2000416 (2021)
18. P. Jóvári *et al.,* Local order in amorphous Ge 2 Sb 2 Te 5 and Ge Sb 2 Te 4. *Phys. Rev. B* **77**, 035202 (2008)
19. J.Y. Raty, C. Otjacques, J.P. Gaspard, C. Bichara, C. Amorphous structure and electronic properties of the Ge1Sb2Te4 phase change material. *Solid State Sci.* **12**, 193-198 (2010)
20. L. Guarneri *et al.,* Metavalent bonding in crystalline solids: how does it collapse? *Adv. Mater*. **33**, 2102356 (2021)